Molecular Crystals and Liquid Crystals
Publication details, including instructions for authors and subscription information:
http://www.tandfonline.com/loi/gmcl18

Local States in One-Dimensional CDW Materials; Spectral Signatures for Polarons and Bipolarons in MX Chains

B. I. Swanson [a], R. J. Donohoe [a], L. A. Worl [a], A. D. F. Bulou [a], C. A. Arrington [a], J. T. Gammel [a], A. Saxena [a] & A. R. Bishop [a]
[a] Los Alamos National Laboratory, Los Alamos, N.M., 87545
Version of record first published: 04 Oct 2006.

To cite this article: B. I. Swanson , R. J. Donohoe , L. A. Worl , A. D. F. Bulou , C. A. Arrington , J. T. Gammel , A. Saxena & A. R. Bishop (1991): Local States in One-Dimensional CDW Materials; Spectral Signatures for Polarons and Bipolarons in MX Chains, Molecular Crystals and Liquid Crystals, 194:1, 43-53

To link to this article: http://dx.doi.org/10.1080/00268949108041149

Mol. Cryst. Liq. Cryst., 1991, vol. 194, pp. 43–53
Reprints available directly from the publisher
Photocopying permitted by license only

Printed in the United States of America

LOCAL STATES IN ONE-DIMENSIONAL CDW MATERIALS; SPECTRAL SIGNATURES FOR POLARONS AND BIPOLARONS IN MX CHAINS

B. I. SWANSON, R. J. DONOHOE, L. A. WORL, A. D. F. BULOU, C. A. ARRINGTON, J. T. GAMMEL, A. SAXENA, AND A. R. BISHOP
Los Alamos National Laboratory, Los Alamos, N.M. 87545

Abstract Defect and ground states in halide-bridged mixed valence platinum chains (MX) have been investigated by absorption and resonance Raman spectroscopies and the results compared with many body Peierls Hubbard calculations. The asymmetry in the excitation profiles for the electron and hole polaronic defects in PtCl and the observation of hole bipolaron defect states with absorption well above the charge transfer band edge confirm the importance of including the halide band in the Peierls-Hubbard Hamiltonian (2-band, 3/4-filled calculations). Tuning the MX materials by mixing chloride and bromide at the bridging halide position results in dramatic increase in the concentration of valence defects (holes and electrons) as well as new edge state defects. In these mixed chain solids, defect state modes that correspond to formerly IR-active vibrations gain Raman intensity by polarization of the sites at the defect boundary. These edge states are observed with Raman excitation above the charge transfer edge and are further verification of the importance of halide band in the electronic properties of the MX materials.

Keywords: Low dimensional solids, charge density wave, gap states, polarons, bipolarons, mixed valence solids

INTRODUCTION

Halide-bridged mixed-valence metal linear chains (HMMCs or MX) are anisotropic solids that exhibit electronic properties dominated by strong electron-phonon and electron-electron interactions.[1] The low-dimensional nature of these materials allows simplification of theoretical modelling and provides a means by which the electronic properties can be experimentally tuned in a predictable manner. This tunability includes alteration of the basic chemical composition of the chain and perturbation of the chain by external forces. The former method is primarily associated with the choice of the metal (M, typically from the platinum group) and bridging halide (X) components and, to a much lesser extent, the ancillary ligands and counterions. As an example, chloride-bridged platinum chains (PtCl) are charge density wave (CDW) materials with the chlorides displaced off the central position toward alternate metal sites. This Peierls distortion leads to oxidation states for the alternate metal sites that approach +2 and +4, a charge transfer band edge near 500 nm and insulating/semiconducting electronic properties.[2] In

contrast, NiBr chains exhibit no Peierls distortion, +3 metal sites, an absorption edge near 1000 nm and antiferromagnetic character suggestive of a spin density wave (SDW) material.[3] In general, the strength of the CDW phase increases for the metal series Ni<Pd<Pt and for the halide series I<Br<Cl.

In addition to chemical tunability, the electronic properties of MX materials can be altered through external perturbations such as application of pressure[4] or defect-inducing approaches such as doping and photolysis.[5] These methods may prove to be fruitful in the search for a metal-insulator transition in HMMCs. In particular, much of the electronic character of HMMCs is determined by the nature and level of defects; these include valence irregularities in the metal sites such as electron and hole polarons (Pt^{III} at sites that are normally Pt^{IV} and Pt^{II}, respectively) and bipolarons (two extra or missing charges) as well as domain walls in which the phase of the CDW (or SDW) may become reversed. Structural defects, such as chain ends, missing counterions or contaminated M or X sites, can also occur.

We have undertaken a combined theoretical and experimental effort directed toward the examination of both the ground and defect states in HMMC materials as they are tuned within and between broken symmetry phases. Novel low-dimensional highly correlated electronic materials offer a difficult theoretical challenge as we must span from a description of electronic structure on a molecular scale to the meso scale structure that is intrinsic to these solids. Our theoretical effort at Los Alamos combines quantum chemistry, band structure calculations, and many body modeling using Peierls-Hubbard Hamiltonians (i.e., incorporating both electron-phonon and electron-electron interactions) in order to model ground and local states. The experimental effort combines synthesis and a variety of microscopic structural and spectroscopic probes and macroscopic measurements in an effort to fully characterize both ground and local states as these materials are tuned in the phase boundary regions between broken symmetry states. The present article summarizes some of our recent research using optical spectroscopy to obtain signatures of photoexcited and intrinsic local states and compares these experimental results with Peierls-Hubbard calculations of the optical properties of these materials. Details concerning the theoretical and experimental approaches can be found elsewhere.[1b,6,7]

PHOTO-INDUCED DEFECT STATES IN PtCl AND THE 2-BAND MODEL

The PtCl solid $[Pt^{II}(en)_2][Pt^{IV}(en)_2Cl_2](ClO_4)_4$ (en=ethylenediamine) has been intensively examined both for ground and defect state properties.[5,7,8,9] Kurita's

group was first to notice that metastable levels of defects can be generated by photolysis of the PtCl crystals within the intervalence charge transfer band (IVCT) at low temperatures.[5] The elevated defect concentration was manifested by increased intensity in the sub-gap defect absorption bands, the so-called A and B bands, that are observed immediately to the red of the IVCT edge, with a concomitant increase in the EPR signal intensity and conductivity. Interestingly, the increased defect levels were reversibly removed upon warming of the sample to room temperature. Because the photo-induced defects are paramagnetic, Kurita tentatively attributed them to polarons that are generated via electron hole pair separation of the excitonic charge transfer state. Confirmation of this assignment was provided by our group when a mid-infrared absorption band (C band) was also observed to gain intensity upon photolysis within the IVCT.[8] The grow-in of this low energy electronic transition and its decay at elevated temperatures mimic the behavior observed by Kurita *et al.* for the A and B bands.[5] This result agrees with the predicted absorption characteristics of polaron defects as modelled by Bishop *et al.*[6] In addition to the electronic absorption features, we observed increased resonance Raman intensity for two sets of defect vibrations.[7] The first set is associated with a peak at 287 cm^{-1} and the second with a peak at 263 cm^{-1}. We noted that an excitonic intermediate might be expected to yield both hole and electron polarons and tentatively assigned the 287 cm^{-1} peak to hole polarons and the 263 cm^{-1} band to electron polarons. Subsequent lattice dynamics calculations[10] support these assignments.

The many-body model Hamiltonian developed by Bishop *et al.*[6] is specific to the MX materials in that it includes both the half-filled metal and filled halide bands. This 3/4-filled, 2-band approach is in contrast to a typical treatment in which only the metal band is considered (1/2-filled 1-band). Several distinct results are generated by the 2-band Hamiltonian. Among these is the prediction of asymmetry in the electronic properties of electron and hole valence defects. The 1-band treatments predict that the electron and hole defect states for polarons are isoenergetic while the proximity of the halide band to the valence portion of the metal band removes this symmetry in the 2-band calculations. We have strong evidence that asymmetry does indeed exist. The enhancement regions for the 287 and 263 cm^{-1} defect modes upon probing the A and B absorption bands are shown in Figure 1.

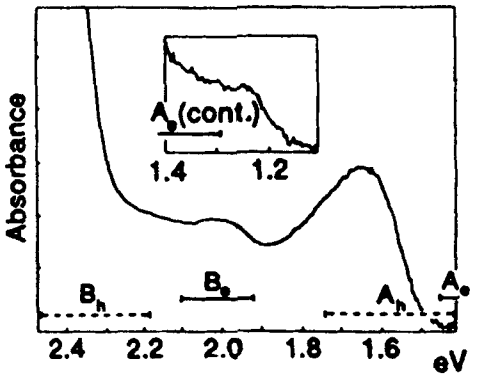

Figure 1. The A and B absorption features for electron (e) and hole (h) polaron defects as determined by resonance enhancement of the 263 and 287 cm^{-1} modes, respectively.

At the red edge of the A band and coincident with the B band, enhancement of the 263 cm^{-1} mode is observed while the 287 cm^{-1} band is enhanced at the maximum of the A band and immediately to the red of the IVCT edge. This ordering of defect states is quantitatively reproduced by the 2-band calculation. Thus, the model of Bishop *et al.*[6] predicts A (gap to gap) and B (gap to band or band to gap) transitions for the PtCl hole (h) and electron (e) polarons in the following order: $A_e<A_h<B_e<B_h$.

Although the 2-band model appears to be quite successful in this matter, asymmetry could be due to preferential pinning of one type of defect at a pre-existing defect site. However, further support for the 2-band model is provided by the experimental observation of absorption features immediately above the IVCT band (ultragap states, see below) that can be attributed to defect state transitions between the halide and metal bands. We are currently examining the ultragap and sub-gap defect states to examine their behavior as a function of the strength of the CDW phase. The 2-band model includes specific predictions with regard to the effects of relaxation of the CDW on defect states.

PtBr, PtI, AND MIXED HALIDE SYSTEMS

Spectral studies of intrinsic and photoexcited states in PtBr and PtI, while presently more limited in scope, have also been performed. PtI has an asymmetric photo-induced absorption feature immediately to the red of the IVCT edge.[11] As is shown in Figure 2, a photo-induced A band like feature can also be observed for PtBr. We find that the energy of this transition is in good agreement with that expected for a polaronic defect.

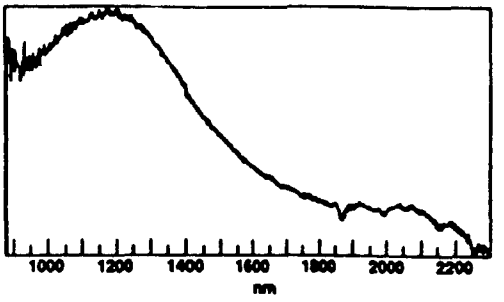

Figure 2. The photo-induced metastable absorption feature for PtBr.

This absorption band, like the A and B bands of PtCl, is stable at low temperature and slowly disappears when the sample is warmed to room temperature. We have also observed increased EPR signals for both PtBr and PtI upon photolysis but have not yet verified that, like the absorption band, these signals are metastable.

Unlike PtCl, the photo-induced EPR signals for PtBr and PtI show no evidence for Pt hyperfine coupling. The photo-induced EPR signals are essentially identical to those reported by Kawamori *et al.* for the unphotolyzed crystals.[12] In addition, both PtI and PtBr demonstrate strong sample dependence in the amount of induced EPR signal; not all samples exhibit this behavior.

Earlier resonance Raman studies of single crystal PtBr at low temperatures showed evidence for complex fine structure in the symmetric stretch chain mode (ν_1) and additional resonance enhanced features as one tuned to the blue of the band edge (ca. 800 nm).[13] These studies demonstrated ν_1 to be comprised of at least five components (168, 171, 174, 177, and 181 cm^{-1}) each with its own excitation profile; the lowest frequency component dominates with excitation near the band edge while the maxima for the excitation profiles for each higher frequency component shift monotonically to the blue. This fine structure was variously attributed to differing correlation lengths along the chain, differing interchain structures, and intrinsic and photo-induced defect states.

Keller *et al.* reported the presence of two types of PtBr crystals, one with an orthorhombic unit cell and one with a monoclinic cell.[14] We have recently studied the sample dependence of the resonance Raman spectra of PtBr and found that the orthorhombic form (all earlier studies had been performed on the monoclinic polymorph) exhibits unusually high relative intensities for modes around 310 cm^{-1}. The frequencies, relative intensities and excitation profile of the fine structure of the feature at 310 cm^{-1} are in remarkable agreement with what is observed for the ν_1 chain mode for pure PtCl. Subsequent NMR studies of the composition of crystals formed using several different synthetic routes showed clear evidence for Cl^- ion

doping in the PtBr samples.[15] In effect, PtCl and PtBr form solid solutions that range in composition from pure PtBr to pure PtCl. Furthermore, the origin of the two different polymorphs of PtBr is a result of the Cl^- ion concentration and a temperature-induced phase transformation from monoclinic to orthorhombic forms that occurs at 292 and 302 K for pure PtCl and PtBr, respectively. Virtually all earlier studies of PtBr have been performed on samples that have substantial Cl^- impurity levels and we believe that this is the source of the very different behavior of photoexcited states in PtCl and PtBr. This inadvertent Cl^- ion doping also gives rise to most of the intense resonance enhanced features in the earlier Raman studies (below).

INTRINSIC AND PHOTO-INDUCED DEFECTS IN PURE PtBr

We have performed resonance Raman studies of PtBr with less than 1% Cl^- impurity where the excitation wavelength has been tuned to the red (750-970 nm) and the blue (750-488 nm) of the IVCT band edge. Spectra obtained with excitation to the red of the band edge (Figure 3) show, in addition to the ν_1 fundamental at 166 cm^{-1} and its overtones, broad features at ca. 150 and 130 cm^{-1}. The maximum in the excitation profile for the 150 cm^{-1} feature is found immediately to the red of the band edge while that for the 130 cm^{-1} feature is further to the red (ca. 1000nm).

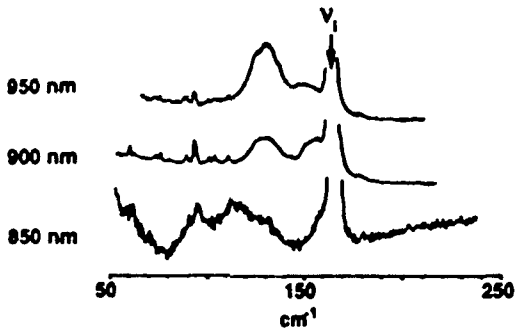

Figure 3. Raman spectra for PtBr (1% Cl) obtained below the IVCT band edge with the listed excitation wavelengths.

On the basis of lattice dynamic calculations for charge defects in PtBr and the calculated absorptions using Peierls-Hubbard models, we attribute the 150 cm^{-1} feature to an electron polaron and the 130 cm^{-1} band to an electron bipolaron. Preliminary studies of the change in the resonance Raman after photoexcitation into the IVCT band indicate that the feature at 130 cm^{-1} grows in intensity.

Raman spectra obtained with excitation to the blue of the IVCT band edge are shown in Figure 4. With excitation in the range 750-600 nm, only the ν_1 fundamental and its overtones are observed. Excitation at 568.2 nm shows evidence for a component at 171 cm^{-1} and additional components at 175 and 181 cm^{-1} appear with excitation further to the blue.

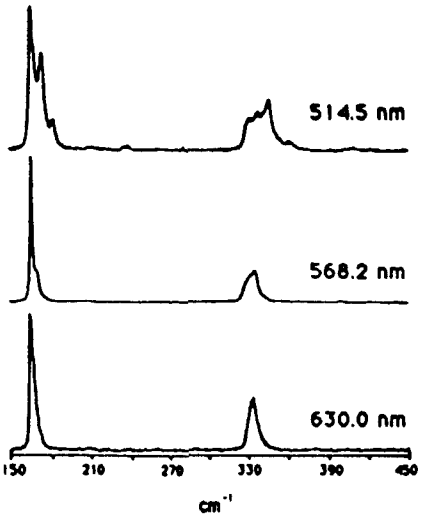

Figure 4. Raman spectra for PtBr (1% Cl) obtained above the IVCT band edge with the listed excitation wavelengths.

While the wavenumber positions for these additional ν_1 components are the same as those observed for samples doped with Cl^-, their excitation profiles are shifted well to the blue. At present, it is not clear whether the components at 171, 175 and 181 cm^{-1} arise from the small residual amount of Cl^- ion left in the sample, from photoexcitation into the IVCT, or are intrinsic to the undoped PtBr lattice. Lattice dynamic calculations do indicate, however, that the Raman modes for hole polarons and bipolarons are expected above the ν_1 fundamental at ca. 181 and 183 cm^{-1}, respectively, and it is likely that hole defects are responsible for the fine structure observed in the ν_1 band upon excitation above the IVCT band in pure PtBr.

Irrespective of the assignment of the features at 171, 175 and 181 cm^{-1} observed in the Raman, it is clear that their excitation profiles and, therefore, their absorption bands are well to the blue of the band edge. The observation of 'ultragap' states (absorptions for defects well to the blue of the band edge) is important as it can only be explained to arise from discrete states pulled from the halide band.[16]

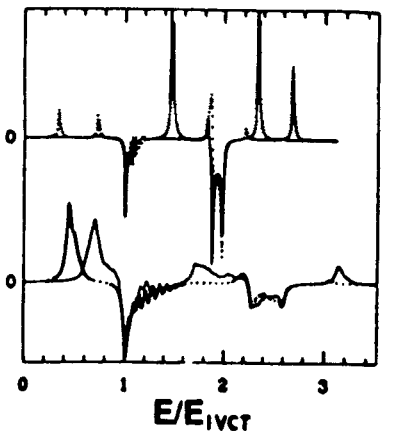

Figure 5. Calculated difference absorption spectra for the MX chains with electron (·····) and hole (——) bipolaron defects. The top spectra are obtained for a strong CDW system and the bottom for a weak CDW system. The abscissa is normalized to the IVCT edge (= 1).

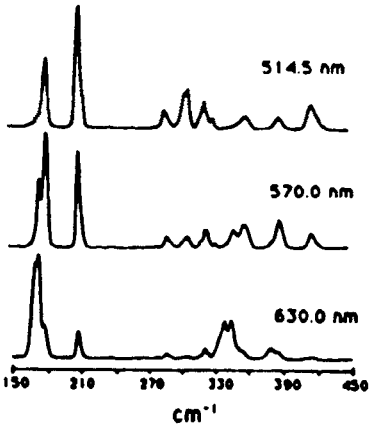

Figure 6. Raman spectra for PtBr (12% Cl) obtained above the IVCT band edge with the listed excitation wavelengths.

Peierls-Hubbard calculations based on a 3/4-filled 2-band model, where the halide bands are explicitly included, are consistent with these observations. Difference spectra calculated via this Peierls-Hubbard approach that correspond to the presence of electron and hole bipolarons are shown in Figure 5. While electron bipolarons for strong CDW solids (PtCl) only show evidence for gap state absorptions, hole bipolarons show a strong absorption in the ultragap region at ca.1.5 of the IVCT band edge.

As the charge disproportionation decreases (towards a weaker CDW such as PtBr) this ultragap absorption broadens and shifts further to the blue and weak ultragap absorptions begin to appear for hole polarons (not shown). On the basis of these Peierls-Hubbard calculations and the lattice dynamics we attribute the resonance Raman features observed well to the blue of the band edge to hole polarons and hole bipolarons.

CHARGE TRANSFER EDGE STATES IN MIXED HALIDE SOLIDS

Resonance Raman studies of mixed halide solids (Cl^- doping in PtBr, Br^- doping in PtCl, and Br^- doping in PtI) show surprisingly complex spectra with numerous defect vibrations in the ultragap region. By way of example, the excitation

dependence to the blue of the band edge for a sample with 12% Cl^- doping in PtBr is shown in Figure 6.

On the basis of concentration dependence studies, photoexcitation studies, Peierls-Hubbard calculations, lattice dynamics, and excitation dependence studies we have assigned the observed Raman modes to specific defect states. These mixed halide systems show a relatively high concentration of charge defects; for Cl^- doped PtBr we observe hole polaron in the PtCl segments of the chains and electron polarons and bipolarons in the PtBr part of the chains. For example, the band at ca. 290 cm^{-1} observed in tuning towards the blue (Figure 6) corresponds to the PtCl hole polaron state.

In addition to charge defects, the mixed halide solids show evidence for edge ultragap states that arise at the interface between differing halide segments along the chains. The mode at 210 cm^{-1} is an example of such an edge state. This mode arises from the bromide part of the lattice and is only observed when Cl^- ion is present in the lattice for PtBr; a similar mode is observed for Br^- doped PtCl and PtI. On the basis of its wavenumber position and lattice dynamic calculations, we attribute this mode to a Raman allowed component of the IR active asymmetric PtBr stretch for a $PtBr_2$ unit that neighbors a Cl^- segment. The strong Raman enhancement observed for this feature is consistent with charge transfer and net polarization of the $PtBr_2$ unit by the neighboring PtCl chain segment.

We have begun to model mixed halide solids in a self consistent manner using the Peierls-Hubbard Hamiltonians developed for the pure PtX solids and, by way of example, present results for PtCl segments in a PtBr chain. The PtCl segment in the model shown here represent four $PtCl_2$ units imbedded in a chain of PtBr. The perturbation of the normal PtBr CDW structure upon addition of a PtCl segment is shown in Figure 7. Within the PtCl segment, the CDW structure is nearly that of a pure PtCl lattice. However, there is a difference in the charge distributions at the interface of the two structures. Note that the reduced Pt site between the two types of lattice appears to nearly mimic the normal PtCl reduced site in terms of charge density. Also, the $PtBr_2$ site nearest the interface has been perturbed by the PtCl lattice in that the metal and the bromide nearest the PtCl segment have become somewhat more positively charged and the bromide nearest the PtBr segment more negatively charged (x10 excess charge lines) with respect to the normal PtBr lattice. Thus, the $PtBr_2$ site near the interface is beginning to manifest the charge distribution within the PtCl structure and is polarized. These charge fluctuations lead to predicted absorption intensity above the normal PtBr IVCT as well as the

unusual resonance enhancement for the *ungerade* IR active PtBr stretch. It is also possible that these interface sites act as pinning sites for valence defects. We are currently investigating the preferred location of valence defects in this scenario as well as one in which the $PtCl_2$ sites are randomly distributed (essentially isolated at low dopant levels) within the lattice.

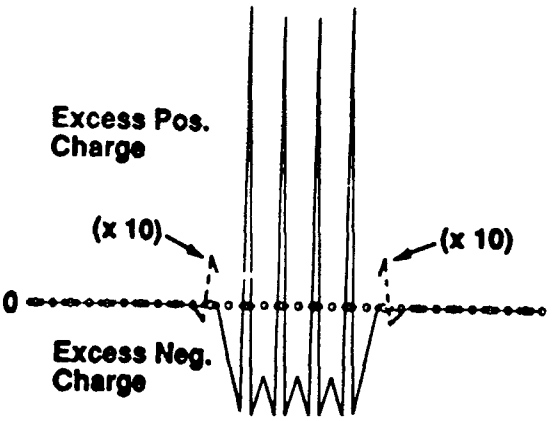

Figure 7. The excess charge density (with respect to the normal PtBr lattice) of a PtCl segment within a PtBr chain. The dashed line indicates where the excess charge density has been multiplied by a factor of 10. The diamonds are the halides and the circles the metals. The 8 Cl^- ions have been darkened to indicate the location of the PtCl domain.

In general, we find charge transfer at the interface to create ultragap edge states and resonances within the IVCT band well to the blue of the band edge. These results are entirely consistent with our resonance Raman studies that show evidence for numerous ultragap states with enhancement of vibration as characteristic of both PtCl and PtBr segments in the mixed halide solids.

CONCLUSIONS

In conclusion, MX solids are novel low-dimensional, strongly correlated electronic materials where the electron-electron and electron-phonon forces can be chemically tuned in the phase boundary region between differing broken symmetry ground states. These materials exhibit a rich spectroscopy for intrinsic, impurity doped, and photoexcited local states that can be modeled using a 2-band Peierls-Hubbard Hamiltonian. We have been able to observe spectral signatures for hole and electron polarons and bipolarons using resonance Raman, infrared and near-IR absorption, and EPR spectroscopies and have found good agreement between these observations and spectral properties calculated using Peierls-Hubbard many-body approaches. We have also observed charge transfer between differing segments of mixed halide chain solids that gives rise to charge and spin defects as well as edge states. In addition to local states with absorptions in the gap region, we have

observed defect states with absorptions in the ultragap region well to the blue of the band edge.

ACKNOWLEDGMENT:

Center for Materials Science and the Materials Science Division for the Office of Basic Energy Science.

REFERENCES

1. (a) J. S. Miller and A. J. Epstein, J. Prog. Inorg. Chem., 20, 1 (1976). (b) D. Baeriswyl and A. R. Bishop J. Phys. C: Solid State Phys., 21, 339 (1988).
2. M. Tanaka, S. Kurita, T. Kojima, and Y. Yamada, Chem. Phys., 91, 257 (1984).
3. K. Toriumi, Y. Wada, T. Mitani, S. Bandow, M. Yamashita, and Y. Fujii, J. Am. Chem. Soc., 111, 2341 (1989).
4. L. V. Interrante, K. W. Browall, and F. P. Bundy, Inorg. Chem., 13, 1158 (1974).
5. S. Kurita and M. Haruki, Syn Metals, 29, F129 (1989).
6. J. T. Gammel, R. J. Donohoe, A. R. Bishop, and B. I. Swanson, J. Phys: Condensed Matter Solid State Phys., submitted for publication.
7. R. J. Donohoe, R. B. Dyer, and B. I. Swanson, Solid State Commun., 73, 521 (1990).
8. R. J. Donohoe, S. A. Ekberg, C. D. Tait, and B. I. Swanson, Solid State Commun., 71, 49 (1989).
9. R. J. Donohoe, C. D. Tait, and B. I. Swanson, Chem. Materials, in press.
10. A. D. F. Bulou, R. J. Donohoe, and B. I. Swanson, manuscript in preparation.
11. N. Matsushita, N. Kojima, T. Ban, and I. Tsujikawa, J. Phys. Soc. Japan, 56, 3808 (1987).
12. A. Kawamori, R. Aoki, and M. Yamashita, J. Phys. C: Solid State Phys., 18, 5487 (1985).
13. S. D. Conradson, R. F. Dallinger, B. I. Swanson, R. J. H. Clark, and V. B. Croud, Chem. Phys. Lett., 135, 463 (1987).
14. (a) H. J. Keller, B. Muller, G. Ledezma, and R. Martin, Acta Cryst., C41, 16 (1985). (b) H. Endres, H. J. Keller, R. Martin, U. Traeger, and M. Novotny, Acta Cryst., B36, 35 (1980).
15. S. C. Huckett, R. J. Donohoe, L. A. Worl, A. D. F. Bulou, C. Burns, and B. I. Swanson, Chem. Materials, submitted for publication.
16. R. J. Donohoe, A. D. F. Bulou, J. T. Gammel, A. R. Bishop, and B. I. Swanson, manuscript in preparation.